scientific reports

Check for updates

OPEN

Comprehensive transcriptomic analysis reveals canonical and novel pathways modulated by nanoceria in mammalian retinal degeneration

L. Donato[1,2,8], D. Zerti[3,8], I. Babiloni-Chust[4], M. Passacantando[5], V. Flati[3], M. Feligioni[6,7], M. Carl[4], C. Rinaldi[1], L. Poggi[4], R. D'Angelo[1]✉ & R. Maccarone[3]

Retinal neurodegenerative diseases such as Age-related Macular Degeneration (AMD) and Retinitis Pigmentosa cause irreversible vision loss due to the limited regenerative capacity of the mammalian retina. Cerium oxide nanoparticles (nanoceria) are emerging therapeutics against oxidative stress and inflammation, major drivers of photoreceptor degeneration, and have demonstrated morphological and functional neuroprotection in preclinical models. However, the genome-wide transcriptional mechanisms underlying these effects remain incompletely characterized. We performed retinal transcriptomic analysis in a rat AMD model induced by intense light and treated intravitreally with nanoceria. Six groups were analyzed: control, light damage, vehicle, nanoceria, vehicle + light damage, and nanoceria + light damage. Light damage activated inflammatory and apoptotic programs, with upregulation of cytokines (*Tnf*, *Il6*, *Il1b*, *Ccl2*) and downregulation of photoreceptor genes (*Rho*, *Pde6a/b*, *Gnat1*). Nanoceria treatment counteracted these effects, suppressing pro-inflammatory mediators, restoring antioxidative genes (*Nfe2l2*, *Gclc*, *Sod2*), and enhancing neuroprotective factors (*Bdnf*, *Cntf*, *Ngf*). Pathway analyses revealed inhibition of TNF/NF-κB/IL-17 signaling and activation of PI3K-Akt, JAK-STAT, and neurotrophin pathways. Unexpectedly, nanoceria also modulated amino acid and insulin metabolism (Ass1, Cps1, Insr, Irs1, Slc2a4) and reactivated transcription factors (Ascl1, Sox2, Notch1) typically silent in adult retina. Our findings highlight nanoceria as a multifunctional therapeutic that mitigates retinal degeneration by coordinating oxidative, inflammatory, and regenerative responses. Together with prior morphological and functional validations, these results support the translational potential of nanoceria for treating retinal neurodegenerative diseases.

Keywords Nanoceria, Retinal degeneration, Transcriptomic analysis, Oxidative stress modulation, Neuroinflammatory modulation, Regenerative responses

Retinal neurodegenerative diseases represent a leading cause of blindness worldwide, with age-related macular degeneration (AMD) and retinitis pigmentosa (RP) affecting millions of patients[1]. Unlike lower vertebrates such as zebrafish that possess remarkable retinal regenerative capacity through Müller glia reprogramming, the adult mammalian retina has minimal intrinsic regenerative potential, making photoreceptors loss irreversible[2]. The pathophysiology of retinal degeneration involves complex interactions between oxidative stress, chronic inflammation, and metabolic dysfunction[3,4]. Acute high-intensity light damage (LD) in rodents reproduces key

[1]Department of Biomedical and Dental Sciences and Morphofunctional Imaging, University of Messina, Messina 98125, Italy. [2]Department of Biomolecular Strategies, Genetics and Cutting-Edge Therapies, I.E.ME.S.T., 90139 Palermo, Italy. [3]Department of Biotechnological and Applied Clinical Sciences, University of L'Aquila, 67100 L'Aquila, Italy. [4]Department of Cellular, Computational and Integrative Biology (CIBIO), University of Trento, 38123 Trento, Italy. [5]Department of Physical and Chemical Sciences, University of L'Aquila, 67100 L'Aquila, Italy. [6]Fondazione European Brain Research Institute (EBRI) Rita Levi-Montalcini, Rome, Italy. [7]Department of Neurorehabilitation sciences, Casa di cura IGEA, Milan 20144, Italy. [8]L. Donato and D. Zerti contributed equally to this work. ✉email: rdangelo@unime.it

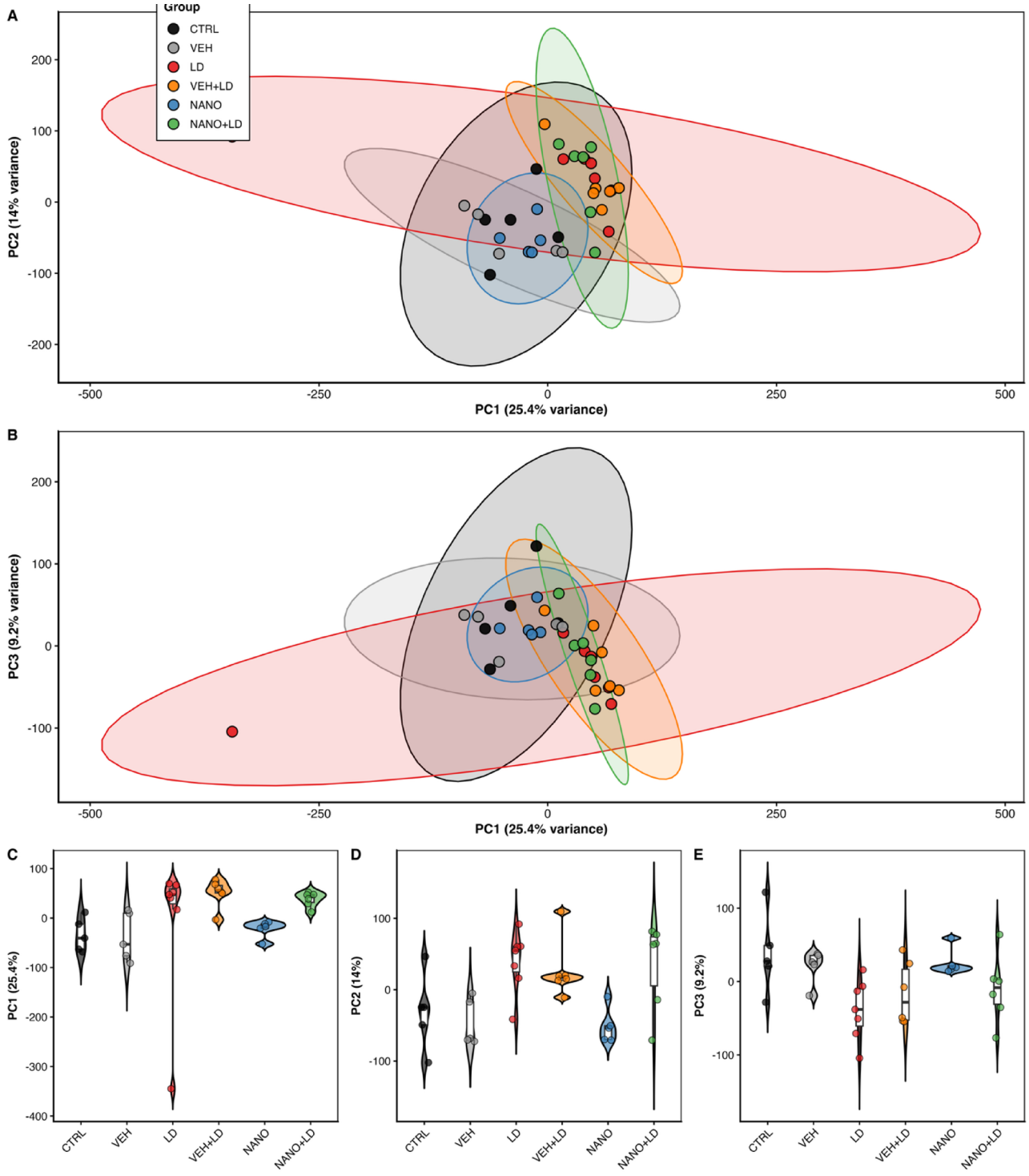

features of photoreceptor degeneration observed in AMD, driven by oxidative stress, inflammatory activation, and apoptosis[5].

Based on our knowledge, cerium oxide nanoparticles (nanoceria) have emerged as promising therapeutics due to their unique redox-switching properties between Ce^{3+}/Ce^{4+} oxidation states, conferring catalytic, self-regenerating free-radical scavenging activity[6,7]. Previous studies demonstrated that intravitreal nanoceria reduce the ROS accumulation, temper microgliosis, preserve photoreceptors, and protect the retinal pigment epithelium in LD paradigms[3,4,6–9]. However, the genome-wide molecular programs engaged by nanoceria in the degenerating mammalian retina remain incompletely defined.

Here we perform bulk RNA-seq in a rat LD model with and without intravitreal nanoceria to systematically map nanoceria-responsive gene networks. We test whether nanoceria not only blunt canonical oxidative-stress and inflammatory pathways but also modulate metabolic and regeneration-linked circuits relevant to photoreceptor survival. By integrating differential expression and pathway enrichment analyses, we provide a transcriptomic framework for nanoceria's mode of action and nominate testable targets for neuroprotective

◀**Fig. 1**. Principal component analysis (PCA) of transcriptomic profiles across experimental groups. (**A**) PCA scatter plot (PC1 vs. PC2) of variance-stabilized RNA-seq data (TPM-normalized) reveals clear transcriptomic segregation among the six experimental groups: control (CTRL, black circles), light damage (LD, red circles), vehicle injection (VEH, gray circles), nanoceria treatment (NANO, blue circles), vehicle + light damage (VEH + LD, orange circles), and nanoceria + light damage (NANO + LD, green circles). Each point represents an individual biological replicate ($n = 5–7$ per group). Shaded ellipses represent 95% confidence intervals for each group. PC1 (explaining 25.4% of total variance) primarily captures the effect of light damage, separating light-damaged samples (LD, VEH + LD, NANO + LD) from non-damaged groups (CTRL, VEH, NANO). PC2 (explaining 14.0% of variance) reflects the nanoceria treatment effect, distinguishing nanoceria-treated samples (NANO, NANO + LD) from their vehicle-treated or untreated counterparts. (**B**) PCA scatter plot (PC1 vs. PC3) provides additional resolution of transcriptomic relationships. PC3 (explaining 9.2% of variance) captures residual biological variability and further separates treatment responses within experimental groups. (**C**–**E**) Violin plots showing the distribution of sample scores along PC1, PC2, and PC3, respectively, highlighting tight clustering of biological replicates within groups and statistically significant separation between experimental conditions (one-way ANOVA: PC1, $F = 3.26$, $p = 0.0075$; PC2, $F = 4.48$, $p = 0.0007$; PC3, $F = 1.81$, $p = 0.113$). PCA was performed on variance-stabilized transformation (log2-transformed TPM values) of normalized count data. Individual data points (jitter) represent biological replicates. Statistical significance assessed by one-way ANOVA with Tukey's post-hoc test. Total samples: $n = 34$ (CTRL = 5, VEH = 5, LD = 7, VEH + LD = 6, NANO = 5, NANO + LD = 6).

therapy in AMD-like injury[5]. We hypothesize that nanoceria not only mitigate inflammatory and oxidative injury but also create a permissive transcriptional environment that may enable partial reactivation of latent regenerative programs in the adult retina.

Results

Light damage activates inflammatory/apoptotic programs and suppresses photoreceptor identity

Principal component analysis (PCA) of $\log_2$-transformed TPM-normalized RNA-seq data revealed clear transcriptomic segregation among all six experimental groups (Fig. 1A, B, Supplementary Table S1). The first principal component (PC1), explaining 25.4% of total variance, primarily captured the transcriptional impact of acute light damage, with light-damaged samples (LD, VEH + LD, NANO + LD) clustering distinctly from non-damaged groups (CTRL, VEH, NANO) along this axis (one-way ANOVA: $F = 3.26$, $p = 0.0075$). The second principal component (PC2, explaining 14.0% of variance) reflected the treatment effect of nanoceria, effectively separating nanoceria-treated samples (NANO, NANO + LD) from vehicle-treated or untreated controls ($F = 4.48$, $p = 0.0007$). The third principal component (PC3, 9.2% variance) captured residual biological variability and further differentiated treatment responses, particularly within the light-damaged cohort ($F = 1.81$, $p = 0.113$).

Importantly, biological replicates within each experimental group clustered tightly ($n = 5–7$ per group; total $n = 34$), indicating high technical reproducibility and robust biological consistency across samples (Fig. 1C–E). Vehicle injection alone (VEH) did not substantially alter the transcriptomic profile relative to untreated controls (CTRL), as evidenced by their close proximity and overlapping confidence ellipses in PCA space. Notably, the NANO + LD group occupied an intermediate position between LD and control groups along PC1, suggesting that nanoceria treatment partially reversed the transcriptional signature induced by light damage. These global transcriptomic patterns are fully consistent with subsequent differential expression analyses, which demonstrate that nanoceria modulate both baseline retinal homeostasis (NANO vs. CTRL) and injury-induced transcriptional programs (NANO + LD vs. LD).

Light damage activates inflammatory/apoptotic programs and suppresses photoreceptor identity

Acute high-intensity light exposure (LD) produced a broad transcriptional shift versus controls (CTRL), with hundreds of DEGs (e.g., ~920 at FDR < 0.05; 666 up/254 down). Upregulated genes encompassed cytokines/chemokines (*Tnf*, *Il6*, *Il1b*, *Ccl2/Ccl3/Ccl4*), gliosis/microglial markers (*Gfap*, *Aif1*), and stress/apoptosis mediators (Bax, Casp3), while photoreceptor and visual-cycle transcripts were prominently reduced (*Rho*, *Pde6a/b*, *Gnat1*, *Cnga1*; transcriptional regulators *Crx*, *Nrl*, *Nr2e3*). Enrichment analyses highlighted TNF/NF-κB and p53/apoptosis among upregulated pathways, with strong depletion of phototransduction and retinol/visual-cycle terms. These data establish the canonical oxidative-inflammatory injury signature and loss of photoreceptor identity in LD (Fig. 2; Table 1; Fig. S1).

Intravitreal vehicle injection exerts minimal transcriptomic impact

Vehicle (VEH) alone induced only minor changes relative to CTRL (dozens of DEGs with small effect sizes and no significant GO/KEGG categories after correction), indicating the injection procedure/vehicle is largely transcriptionally inert at the assayed time point. Similarly, VEH-LD vs. LD showed only subtle and inconsistent differences, confirming that injection does not confound the LD injury signature (Supplementary Fig. S2–S3; Supplementary Tables S4–S5).

In uninjured retina, nanoceria prime a cytoprotective mitochondrial/antioxidant state

Nanoceria treatment in healthy eyes (NANO vs. CTRL) reprogrammed the transcriptome toward oxidative-stress resilience and metabolic competence. Antioxidant master regulator *Nfe2l2* (*Nrf2*) and canonical targets (*Hmox1*,

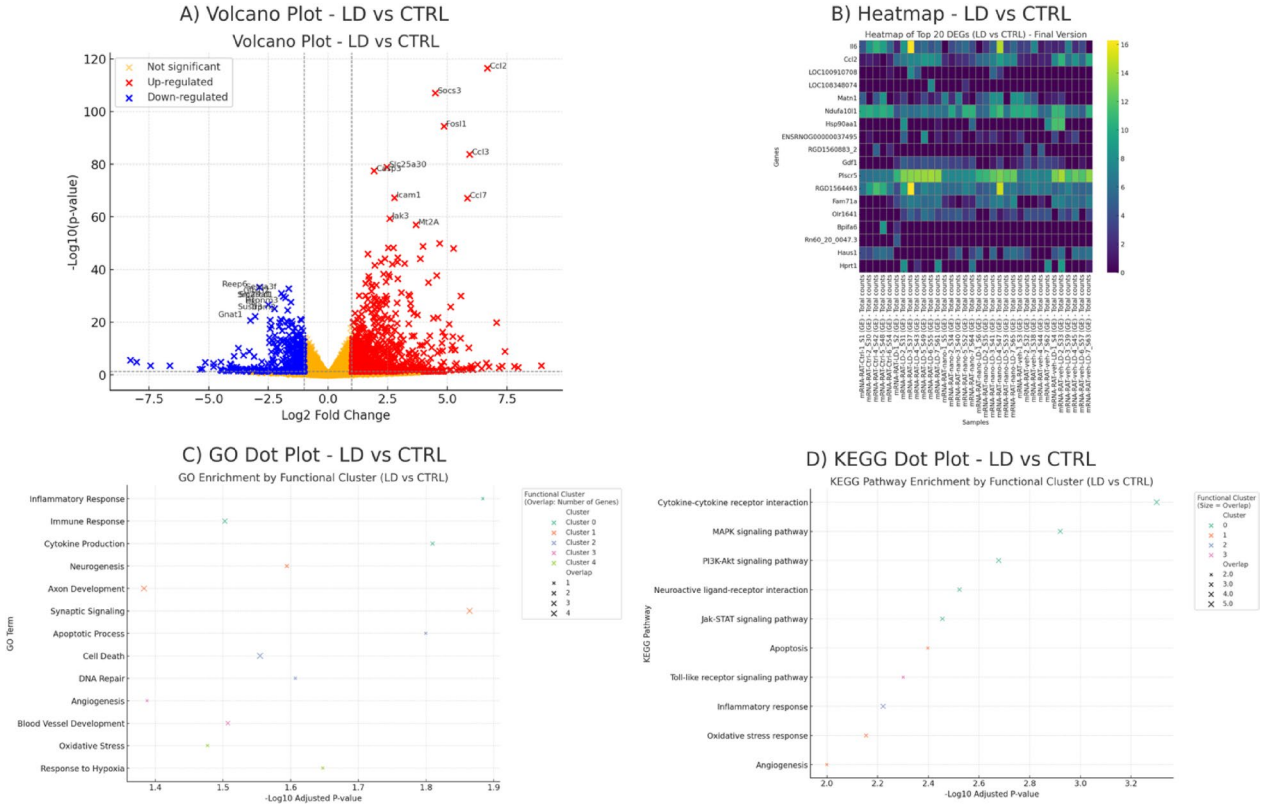

Fig. 2. Light damage (LD) activates inflammatory/apoptotic programs and suppresses phototransduction. (**A**) Volcano plot for LD vs. CTRL (FDR < 0.05) highlighting upregulation of cytokines/chemokines (e.g., *Tnf*, *Il6*, *Il1b*, *Ccl2/Ccl3/Ccl4*) and gliosis markers, with strong downregulation of photoreceptor/visual-cycle transcripts (e.g., *Rho*, *Pde6a/b*, *Gnat1*, *Cnga1; Crx*, *Nrl*, *Nr2e3*). Log_2 fold-change values are apeGLM-shrunken estimates. Red/blue points indicate significantly upregulated/downregulated genes, respectively. (**B**) Heatmap of top DEGs illustrates clear CTRL vs. LD segregation. (**C**, **D**) Summary enrichment (GO/KEGG) indicates upregulation of inflammatory response/TNF–NF-κB/apoptosis and downregulation of phototransduction/retinol metabolism; full enrichment in Fig. S1. Differential expression determined with DESeq2, using Wald test and Benjamini–Hochberg correction. Significance defined at adjusted p (FDR) < 0.05. Sample size: $n = 6$ biological replicates per group.

Nqo1, *Gclc*, *Sod2*, *Gpx family*, *Prdx1*) were induced, alongside mitochondrial/OXPHOS and bioenergetic genes (*Idh3a/b*, *Cpt1a*, *Acat2*, *Ppargc1a*). In parallel, inflammatory and apoptotic transcripts (*Tnf*, *Il1b*, *Nlrp3*, *Casp3*, *Bax*) were reduced. These data support a "preventive" effect whereby nanoceria elevate antioxidant capacity and mitochondrial organization while dampening basal inflammatory tone (Fig. S4–S5; Supplementary Table S5).

In injured retina, nanoceria reverse degeneration signatures and enhance survival/trophic programs

In LD eyes, nanoceria (NANO-LD) broadly opposed the injury signature relative to LD alone. Damage-induced inflammatory mediators and gliosis markers (e.g., *Tnf*, *Il6*, *Il1b*, *Ccl2*, *Nfkbia*, *Gfap*, *Aif1*) were strongly reduced, while photoreceptor transcripts (*Rho*, *Pde6b*) were preserved/partially restored. Nanoceria concomitantly induced neuroprotective and trophic factors (*Bdnf*, *Cntf*, *Ngf*, *Sirt1*) and regeneration-linked regulators (*Ascl1*, *Sox2*, *Notch1*, *Wnt2b*), indicating transcriptional reversal of injury-induced pathways. Pathway analyses showed suppression of TNF/NF-κB/IL-17 and activation of PI3K–Akt, JAK–STAT, neurotrophin signaling, with strengthened oxidative phosphorylation and mitochondrial organization (Fig. 3; Table 2; Supplementary Fig. S6, Supplementary Table S6). Direct comparison against vehicle in LD (NANO-LD vs. VEH-LD) confirmed these nanoceria-specific effects (Fig. 4). Together, these results indicate that nanoceria both quell inflammatory/apoptotic cascades and engage pro-survival networks that promote transcriptomic recovery.

Nanoceria uncover "non-canonical" axes: amino-acid/urea-cycle and insulin/glucose signaling

Beyond antioxidant and inflammatory pathways, nanoceria modulated amino-acid metabolism/urea-cycle genes (e.g., *Ass1*, *Cps1*, *Otc*), reversing their LD-associated repression and elevating expression toward or above baseline, consistent with enhanced nitrogen handling and anaplerotic support. In parallel, nanoceria increased insulin/IGF signaling components (*Insr*, *Irs1*) and the insulin-responsive glucose transporter *Slc2a4* (Glut4), suggesting improved glucose utilization and coupling to PI3K–Akt survival signaling in stressed retina. These

Gene	log_2FC	FDR	Gene	log_2FC	FDR
LD vs. CTRL — Top up-regulated (left) and down-regulated (right)					
Hprt1	8.95	4.2e−03	*Rn60_20_0047.3*	− 8.29	6.6e−05
Hsp90aa1	7.97	1.6e−02	*RGD1560883_2*	− 7.98	1.1e−02
LOC108348074	7.82	6.9e−03	*Matn1*	− 7.57	5.4e−03
Fam71a	7.42	7.3e−08	*ENSRNOG00000046377*	− 7.35	1.8e−02
Olr1641	7.29	5.9e−03	*Gdf1*	− 7.34	3.2e−07
Haus1	7.17	2.0e−02	*Ndufa10l1*	− 7.26	2.5e−02
Il6	7.07	2.5e−18	*LOC108348155*	− 7.20	1.2e−02
Plscr5	6.74	9.3e−03	*RGD1564463*	− 7.15	7.7e−03
Ccl2	6.68	7.6e−113	*Bpifa6*	− 6.99	1.1e−06
ENSRNOG00000037495	6.63	7.1e−04	*LOC100910708*	− 6.71	1.1e−02
NANO-LD vs. LD — Top up-regulated (left) and down-regulated (right)					
Yme1l1	8.24	1.4e−02	*LOC100909505*	− 10.51	2.3e−03
AABR07065782.1	7.52	2.9e−02	*LOC100909505 (iso)*	− 9.38	2.7e−03
AABR07060963.1	7.16	1.3e−02	*Ccl2*	− 7.17	2.0e−02
Ngf	6.88	3.8e−02	*Cd14*	− 6.62	3.3e−02
Bdnf	6.70	4.9e−02	*Il6*	− 6.50	2.9e−02
Sirt1	6.55	3.2e−02	*C1qb*	− 6.33	3.5e−03
Mt1	6.33	1.8e−02	*Tnf*	− 6.12	4.8e−02
LOC689527	6.25	4.5e−02	*Nfkbia*	− 5.90	4.4e−02
Nfe2l2 (Nrf2)	6.10	3.1e−02	*Serpine1*	− 5.80	4.6e−02
Cntf	5.98	2.4e−02	*Lyz2*	− 5.75	2.2e−02

Table 1. Consolidated "Top DEGs" for the two pivotal contrasts. Top up- and down-regulated genes for LD vs. CTRL and NANO-LD vs. LD (ranked by $|log_2FC|$; FDR < 0.05). Complete DEG lists for all five contrasts are provided in supplementary tables S2–S6.

axes were not appreciably engaged by vehicle and represent novel, testable mechanisms by which nanoceria may stabilize retinal bioenergetics (Supplementary Fig. S7; Supplementary Table S7).

qRT-PCR validates key signatures

Targeted qRT-PCR corroborated RNA-seq trends: *Il6* rose after LD and decreased with nanoceria, whereas *Sod2* and *Nfe2l2* increased with LD and remained elevated under nanoceria, consistent with reinforced antioxidant defense. RNA-seq vs. qPCR values showed strong concordance (e.g., Pearson's $r \approx 0.90–0.97$ across genes; $p < 0.05$), supporting dataset robustness (Fig. 5).

Discussions

The current transcriptomic analysis reveals that nanoceria suppress inflammatory and oxidative stress pathways while enhancing antioxidant, metabolic, and regenerative gene networks. These findings extend previous histological and functional evidence[8–13] by providing mechanistic insight into nanoceria's multifaceted neuroprotective action.

Beyond their catalytic antioxidant properties, our findings suggest that nanoceria modulate the retinal microenvironment at the transcriptional level in a way that suppresses injury while simultaneously enabling reactivation of genes typically associated with developmental or regenerative processes.

Rather than acting as passive ROS scavengers[14,15], nanoceria appear to engage upstream transcriptional programs that recondition the degenerating retina and shift the balance toward resilience and repair. Their long-lasting antioxidant activity and favorable safety profile in preclinical models[12,16,17] further support their potential as next-generation, multifunctional therapeutics for retinal disease.

Among the most unexpected and clinically relevant findings, we observed that nanoceria modulate several non-canonical metabolic pathways, including amino acid catabolism, the urea cycle, and insulin/glucose signaling. Genes such as Ass1 and Cps1, which are involved in nitrogen detoxification and arginine metabolism, were suppressed by light damage and restored by nanoceria, suggesting that metabolic reprogramming is a critical aspect of retinal stress adaptation[18,19].

In parallel, nanoceria upregulated Insr, Irs1, and Slc2a4, pointing to reactivation of insulin signaling—a pathway increasingly recognized in retinal degeneration[20]. These metabolic effects may improve glucose utilization and support bioenergetic demands through the PI3K–Akt axis while alleviating inflammatory-metabolic stress crosstalk[21,22].

These transcriptional changes have not previously been associated with nanoceria and position them as modulators of cellular metabolism in addition to their well-known redox properties. Addressing metabolic dysfunction alongside oxidative stress may represent a promising multi-targeted strategy for retinal neuroprotection.

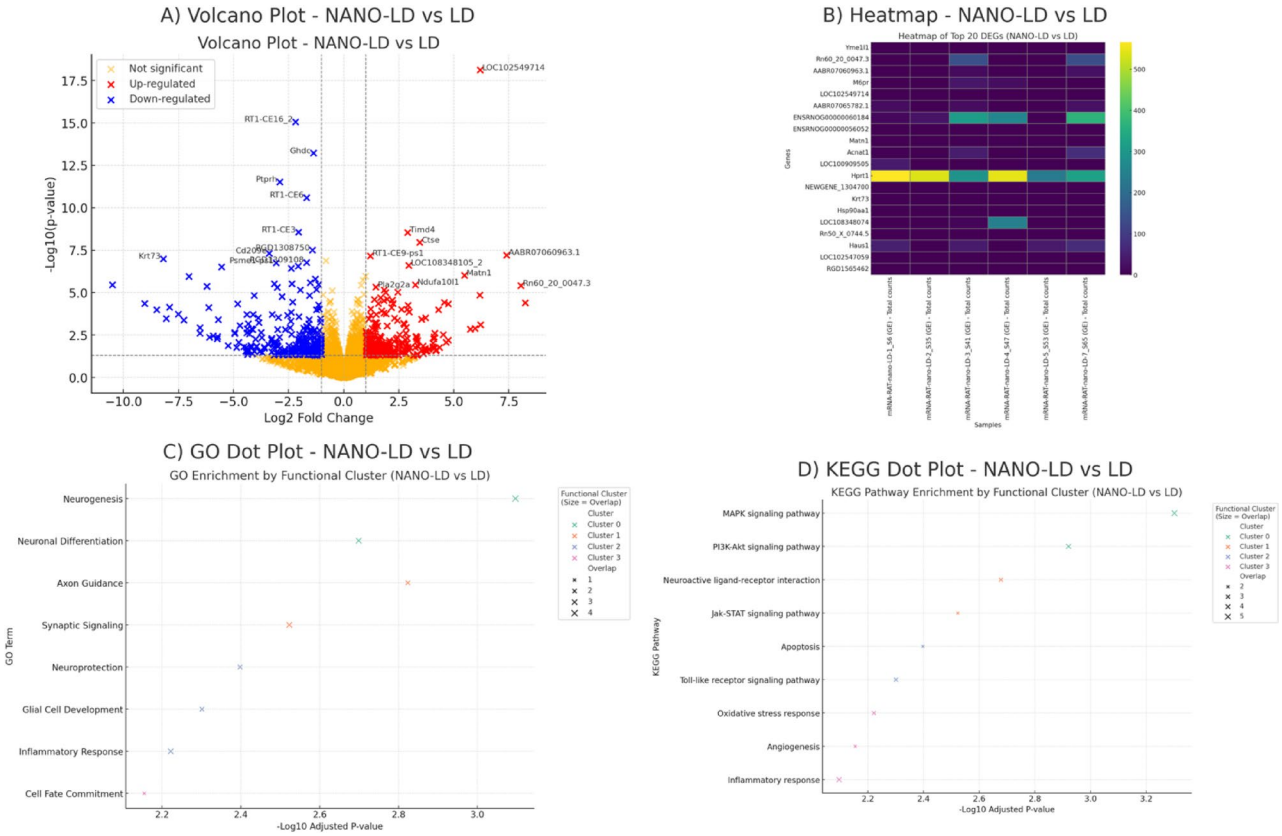

Fig. 3. In injured retina, nanoceria oppose LD-induced signatures and enhance pro-survival networks. (**A**) Volcano for NANO-LD vs. LD (FDR < 0.05) shows downregulation of inflammatory mediators (*Tnf*, *Il6*, *Il1b*, *Ccl2*, *Nfkbia*) and gliosis markers (*Gfap*, *Aif1*) with preservation/recovery of photoreceptor transcripts (Rho, Pde6b). Log_2 fold-change values are apeGLM-shrunken estimates. Red/blue points indicate significantly upregulated/downregulated genes, respectively. (**B**) Heatmap of representative DEGs. (**C**, **D**) Pathway summaries indicate suppression of TNF/NF-κB/IL-17 and activation of PI3K–Akt, JAK–STAT, neurotrophin signaling, alongside strengthened oxidative phosphorylation and mitochondrial organization (full enrichment: Fig. S6). Differential expression determined with DESeq2, using Wald test and Benjamini–Hochberg correction. Significance defined at adjusted p (FDR) < 0.05. Sample size: $n = 6$ biological replicates per group.

Comparison	Significant DEGs (Up/Down)	Key Enriched Pathways (GO/KEGG)
LD vs. CTRL	920 (666 ↑/254 ↓)	↑ Inflammatory response, apoptosis, NF-κB, TNF signaling; ↓ phototransduction, metabolic genes
VEH vs. CTRL	38 (17 ↑/21 ↓)	No significant pathways (minimal changes)
VEH-LD vs. LD	75 (35 ↑/40 ↓)	Subtle ↑ wound response (e.g., Rptn); ↓ complement system (not significant)
NANO vs. CTRL	306 (243 ↑/63 ↓)	↑ Antioxidant activity, mitochondrial metabolism; ↓ apoptosis (caspase activation)
NANO-LD vs. LD	78 (36 ↑/42 ↓)	↑ Neurotrophin signaling, Notch, antioxidant pathways; ↓ NF-κB/TNF signaling, inflammasome
NANO-LD vs. VEH-LD	34 (17 ↑/17 ↓)	↑ Synaptic plasticity, PI3K/Akt, oxidative phosphorylation; ↓ chemokines, cytokines, complement

Table 2. Summary of differential expression and enriched pathways across Comparisons. For each comparison, the table reports the total number of significant differentially expressed genes (DEGs) with the count of up- (↑) and down-regulated (↓) genes, alongside the key significantly enriched gene ontology (GO) terms and KEGG pathways.

Collectively, these properties reinforce the therapeutic value of nanoceria as a next-generation, long-acting neuroprotective nanomedicine for retinal disease.

A principal mechanism by which nanoceria exert neuroprotection in the retina is through attenuation of oxidative stress and suppression of inflammatory signaling cascades. Retinal degenerative diseases—including age-related macular degeneration (AMD), retinitis pigmentosa (RP), and diabetic retinopathy—are driven by chronic oxidative damage and persistent low-grade inflammation that promote photoreceptor apoptosis and retinal pigment epithelium (RPE) dysfunction[23]. Nanoceria, via redox-active Ce^{3+}/Ce^{4+} cycling, act as self-regenerating antioxidants capable of neutralizing superoxide, hydrogen peroxide, and peroxynitrite[24,25].

Fig. 4. Nanoceria vs. vehicle in LD directly demonstrates nanoceria-specific effects. Compact pathway bar/dot plot for NANO-LD vs. VEH-LD emphasizes stronger suppression of inflammatory pathways and enhanced activation of survival/metabolic programs under nanoceria compared with saline. Full volcano/heatmap and enrichment details are in Fig. S7. Differential expression determined with DESeq2, using Wald test and Benjamini–Hochberg correction. Significance defined at adjusted p (FDR) < 0.05. Sample size: $n = 6$ biological replicates per group.

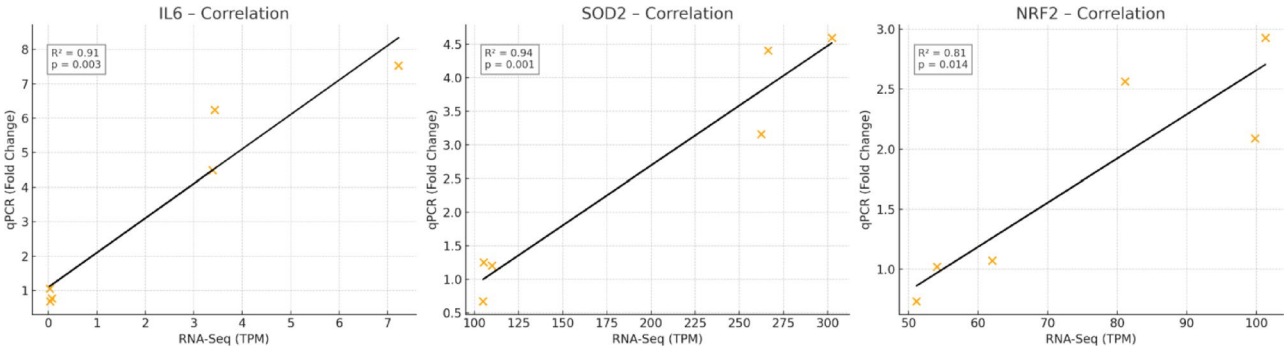

Fig. 5. Correlation between RNA-Seq and qRT-PCR expression for *Il6*, *Sod2*, and *Nrf2*. Scatter plots show a strong concordance between transcriptomic and qPCR data across treatment groups. Expression values from RNA-Seq (TPM) are plotted against corresponding qPCR fold changes. All genes demonstrated robust and statistically significant linear correlations ($R^2 > 0.80$; $p < 0.05$), confirming the consistency of differential expression profiles between the two methodologies. $n = 6$ animals per group, reactions in technical triplicate.

Consistent with our earlier immunohistochemical findings, which demonstrated reduced Iba1-positive microglial activation and decreased inflammatory markers[8,10], the present transcriptomic analysis reveals that nanoceria markedly downregulates proinflammatory genes (*Tnf*, *Il1b*, *Il6*, *Ccl2*) in light-damaged retinas, further supporting its anti-inflammatory mode of action. At the signaling level, we observed decreased expression of *Tlr4* and Myd88, consistent with inhibition of the Toll-like receptor (TLR)–mediated NF-κB pathway. This pathway is a well-established trigger of inflammatory transcriptional programs and microglial activation in retinal degeneration. Supporting this, previous studies demonstrated that cerium oxide nanoparticles attenuate TLR4/NF-κB activation in brain inflammation models, reducing cytokine production and microgliosis[26]. In retinal tissue specifically, Badia et al. [27] demonstrated that CeO_2-NPs reduce microglial activation and suppress TNF-α expression following oxidative stress. These anti-inflammatory effects appear selective and non-immunosuppressive. Instead of silencing broad immune responses, nanoceria specifically interrupt pathological inflammatory cycles while preserving beneficial immune functions such as phagocytosis and matrix remodeling. For instance, in our dataset, *Timd4* and *Ctse*—genes involved in apoptotic cell clearance and lysosomal remodeling—were upregulated, indicating enhanced homeostatic responses. Nanoceria's antioxidant action further complements this immunomodulatory profile. By lowering ROS levels, nanoceria suppress upstream NF-κB activators such as oxidized mitochondrial DNA and lipid peroxidation products[24]. We also observed activation of Nrf2 signaling (Nfe2l2), a master regulator of redox balance. Nanoceria-treated retinas exhibited significant upregulation of canonical Nrf2 target genes: *Hmox1*, *Gclc*, *Nqo1*, and *Sod2*, aligning with prior evidence of Nrf2-mediated neuroprotection by cerium nanoparticles[16,25]. This coordinated suppression of TLR4–MyD88–NF-κB and enhancement of Nrf2-driven antioxidant defense supports a dual mechanism by which nanoceria modulate inflammation and oxidative injury in the retina. Such combined action may be especially advantageous in retinal diseases where these pathways are interlinked in a self-amplifying loop. Our transcriptomic data reinforce this model. Chemokine genes *Ccl2*, *Ccl3*, and *Cxcl10*, which are known drivers of neuroinflammation in light-damaged retinas, were significantly downregulated by nanoceria. Notably, Ccl2 is a key mediator of microglial recruitment and photoreceptor apoptosis[28], while Ccl3 and Cxcl10 participate in chemokine-driven neurodegeneration[29]. Proinflammatory cytokines Il6 and Tnf followed expected dynamics: induced after photic injury and suppressed by nanoceria. These cytokines are well-characterized effectors of gliosis and retinal damage. The glial stress marker *Gfap*, upregulated during Müller cell activation, was also reduced by nanoceria, indicating mitigation of reactive gliosis[28]. Conversely, the neuroprotective factor *Fgf2* remained elevated in nanoceria-treated groups, in line with its role in photoreceptor survival[30]. Downregulation of *Aif1* (IBA-1), a microglial activation marker, further supports nanoceria's capacity to suppress innate immune activation[3]. These transcriptomic signatures strongly support the view that nanoceria modulate the oxidative stress–inflammation axis in a precise and therapeutically favorable manner, reinforcing their potential as neuroprotectants in retinal disease.

Nanoceria neuroprotective activity extends beyond antioxidative effects and includes direct modulation of apoptosis, stress response, and pro-survival pathways. Multiple transcriptomic and qPCR studies have demonstrated that nanoceria treatment downregulates pro-apoptotic genes such as *Casp3*, *Bax*, and *Il1b*, while promoting expression of pro-survival factors including *Bcl2*, *Sirt1*, and neurotrophic genes like *Bdnf*, *Cntf*, and *Ngf*[31]. These changes correlate with delayed photoreceptor cell death and preservation of retinal architecture observed in histological analyses. In the present study, we observed significant suppression of *Casp3*, *Il1b*, *Tnf*, and *Nlrp3* following nanoceria treatment in the LD model, both in direct comparisons and pathway enrichment. These effects were accompanied by the activation of *Nrf2* (*Nfe2l2*) and its downstream targets *Hmox1*, *Gclc*, and *Nqo1*, key components of the antioxidant defense system. The role of Nrf2 in protecting against oxidative and proteotoxic stress in neurons and glia has been firmly established, and it represents a viable therapeutic target in AMD and Parkinson's disease[32]. Importantly, nanoceria-mediated activation of Nrf2 has also been associated with improved mitochondrial quality control. In dopaminergic neurons, CeO_2 nanoparticles reduce mitochondrial fragmentation by inhibiting DRP1 hyperactivation and peroxynitrite formation[31]. Consistently, prior ultrastructural analyses revealed preserved mitochondrial morphology in nanoceria-treated retinas, contrasting with the disrupted, swollen mitochondria observed in untreated LD eyes[33,34]. Transcriptomic analysis further revealed upregulation of stress-responsive transcription factors *Atf3* and *Sirt1*, both associated with cellular recovery following oxidative and metabolic insults. Sirt1, in particular, is known to support mitochondrial biogenesis, energy homeostasis, and antioxidant defense by interacting with FoxO and PGC-1α pathways[32]. The observed increase in *Sirt1* expression in treated animals may synergize with *Nrf2* to promote neuroprotection, especially in the high-energy-demand environment of photoreceptors. An unexpected finding was the upregulation of regeneration-associated transcription factors such as *Ascl1*, *Sox2*, and *Notch1* in nanoceria-treated retinas. These factors are typically quiescent in the adult mammalian retina but are central to the Müller glia reprogramming network in regenerative species like zebrafish[35]. Their re-expression in this context suggests that nanoceria may induce a transcriptional "priming" effect, rendering the retina more responsive to potential regenerative cues. Although histological analysis did not reveal active regeneration or Müller cell proliferation, the transcriptional activation of these genes is noteworthy and may offer a window of opportunity for synergistic therapeutic interventions (e.g., gene therapy or trophic factor delivery). Taken together, our results underscore nanoceria's multifaceted action on survival and stress-response mechanisms. This includes suppression of inflammation and apoptosis, enhancement of antioxidant and mitochondrial defense via Nrf2 and Sirt1, and activation of latent regenerative programs. These concerted transcriptomic changes shift the degenerating retina from a trajectory of degeneration toward stabilization and potentially recovery.

One of the most compelling emerging mechanisms by which nanoceria exert neuroprotective effects is their ability to stabilize autophagy and preserve mitochondrial function—two closely linked processes essential for retinal health. Chronic oxidative stress, a hallmark of retinal degenerative diseases such as AMD and RP, disrupts autophagic flux and promotes mitochondrial dysfunction, leading to bioenergetic collapse and cell

death, particularly in metabolically demanding tissues like the retina and RPE[36]. Recent studies have highlighted nanoceria role in preserving autophagic homeostasis. For example, in a light-damage-induced retinal degeneration model, intravitreal nanoceria treatment prevented abnormal accumulation of LC3B-II and p62 proteins in RPE cells, indicative of restored autophagic flux. Notably, nanoceria blocked aberrant nuclear localization of LC3B—a feature associated with impaired autophagosome maturation and epithelial-mesenchymal transition (EMT) in degenerating RPE[37]. By maintaining normal autophagy, nanoceria preserved RPE integrity and prevented cell death. Complementing these molecular findings, ultrastructural evidence from previous studies demonstrates that nanoceria-treated retinas maintain mitochondrial integrity after injury[38]. These observations align with prior work in neurodegenerative models where nanoceria localized to mitochondria and prevented excessive fission by inhibiting DRP1 hyperactivation, a key step in the mitochondrial apoptotic cascade[39]. Mechanistically, nanoceria appear to exert these effects through multiple routes:

(1) Direct ROS scavenging, reducing mitochondrial oxidative burden;
(2) Suppression of inflammation that can secondarily impair mitophagy;
(3) Stabilization of Nrf2 signaling, which indirectly supports mitochondrial biogenesis and autophagy-related gene expression (e.g., PINK1, Parkin)[40].

Indeed, transcriptomic data from our model show that genes involved in mitochondrial dynamics—Opa1, Mfn1, and Tomm20—were better preserved in nanoceria-treated retinas, suggesting maintenance of mitochondrial fusion and protein import systems. This preservation of mitochondrial and lysosomal health is significant. In AMD, defective autophagy and impaired mitophagy contribute to RPE degeneration, lipofuscin accumulation, and drusen formation. Therapies that restore autophagic flux and mitochondrial clearance—such as rapamycin or metformin—have shown benefit in animal models, but often with systemic side effects. Nanoceria, by contrast, provide a local, long-acting alternative that appears to accomplish similar outcomes through redox modulation and transcriptional reprogramming without systemic toxicity. In sum, the impact of nanoceria on autophagy and mitochondrial maintenance adds a crucial dimension to their neuroprotective repertoire. By targeting fundamental organelle-level processes that govern cell survival, nanoceria go beyond antioxidant action and engage with the core bioenergetic and proteostatic machinery of retinal cells. This capacity to stabilize intracellular quality control systems, particularly under stress, likely underlies the long-term structural and functional protection observed in treated retinas.

Taken together, our data demonstrate that nanoceria exert a multi-dimensional effect on the degenerating retina by attenuating inflammatory mediators (e.g., Tnf, Il1b, Il6, Ccl2), preserving neuroprotective and metabolic gene expression (*Bdnf*, *Cntf*, *Sirt1*, *Nfe2l2*), and reactivating transcriptional programs typically silent in the adult retina. In addition to the expected antioxidant and anti-inflammatory responses, we observed novel transcriptional signatures, including upregulation of amino acid metabolism and urea cycle genes (*Cps1*, *Ass1*, *Otc*), insulin/IGF signaling components (*Insr*, *Irs1*, *Slc2a4*), and regenerative transcription factors (*Ascl1*, *Sox2*, *Notch1*).

These results suggest that nanoceria not only suppress degeneration-associated cascades but also promote a reparative transcriptional landscape. This neuroprotective effect may create a permissive environment for regeneration. A potential limitation of our study is the use of bulk RNA-sequencing, which provides an averaged view of gene expression across all retinal layers and cell types. However, this approach was chosen based on previous literature demonstrating that LD-induced injury is largely confined to the outer retina, particularly the ONL and RPE, and engages a limited number of key cellular players—most notably photoreceptors, Müller glia, and microglia. In this context, bulk RNA-seq is well-suited to detect broad transcriptional programs relevant to damage and repair and has enabled the identification of nanoceria-responsive pathways involved in oxidative stress, metabolism, and regeneration. These results now provide a strong rationale for future single-cell or spatial transcriptomic studies specifically targeting these responsive cell populations.

Conclusions and future directions

Our transcriptomic analysis provides compelling evidence that cerium oxide nanoparticles (nanoceria) elicit a multifaceted neuroprotective response in the retina under both homeostatic and degenerative conditions. In a rat model of light-induced retinal degeneration, nanoceria administration not only attenuated classical markers of oxidative stress and inflammation but also preserved metabolic signaling pathways, restored components of cellular homeostasis, and induced elements of developmental and regenerative transcriptional programs. At the molecular level, nanoceria-treated retinas exhibited reduced expression of genes encoding pro-inflammatory mediators such as TNF-α, IL-6, and CCL2, alongside downregulation of the TLR4–MyD88–NF-κB signaling axis, which is often implicated in retinal and neuroinflammatory pathologies. Concomitantly, we observed the activation of survival-promoting pathways such as PI3K/Akt, neurotrophin signaling, and antioxidant networks under control of *Nfe2l2* (*Nrf2*). Unexpectedly, nanoceria also restored the expression of metabolic regulator genes like *Insr* and *Glut4*, and modulated amino acid and nitrogen metabolism (e.g., ASS1 and CPS1), pointing to novel roles in sustaining retinal bioenergetics and limiting toxic metabolic byproducts. Furthermore, nanoceria triggered the expression of genes typically associated with retinal regeneration in lower vertebrates (e.g., *Notch1*, *Sox2*, *Ascl1*), suggesting that even in the adult mammalian retina, nanoceria may partially reawaken latent regenerative programs. While true neurogenesis was not observed histologically, the transcriptional reprogramming indicates a shift toward a reparative retinal environment—a finding with major implications for regenerative therapeutics. From a translational perspective, these results reinforce the broad-spectrum potential of nanoceria as a next-generation therapy for retinal degenerative diseases such as AMD and RP. Their intrinsic

regenerative redox cycling enables persistent antioxidant activity, and recent advances in delivery platforms (e.g., eye drops, sustained-release hydrogels, intranasal administration) support their clinical feasibility. Importantly, no overt toxicity has been observed in long-term in vivo models, and multiple independent studies across neurodegenerative systems (retina, brain) confirm their efficacy and safety. In conclusion, nanoceria represent a promising disease-modifying agent capable of intervening at multiple levels of retinal degeneration—quenching oxidative and inflammatory cascades, preserving cellular metabolism, and possibly priming repair pathways. This sequential interplay—first quenching stress and inflammation, then initiating regenerative transcriptional activity—highlights a two-stage therapeutic paradigm that merits further investigation. These insights expand our understanding of nanoceria's mode of action and lay the groundwork for future preclinical and clinical studies aimed at establishing nanoceria-based interventions as a therapeutic approach in ophthalmology and beyond.

Methods

Animal model and ethical approval

Adult albino Sprague–Dawley rats (≈2–3 months old, males) were used for all experiments. Rats were born and raised under dim cyclic lighting (12 h light/12 h dark) at constant temperature (~22 °C) and humidity, with diurnal light ≈ 5 lx. Food (standard pellet diet) and water were provided ad libitum. Animals were randomly assigned to experimental groups ($n = 6$ per group) including untreated controls, light-damaged (LD) only, and nanoceria-treated + LD groups (additional vehicle-injected controls were included for injection procedures). All experiments adhered to the ARVO Statement for the Use of Animals in Ophthalmic and Vision Research and the European Directive 2010/63/EU and were approved by the Italian Ministry of Health (authorization no. 763/2020-PR). The authors complied with the ARRIVE guidelines. All efforts were made to minimize animal suffering and to reduce the number of animals used in accordance with the 3Rs principle. To better clarify the experimental design, the seven experimental groups are summarized in Table 3.

Then, to induce retinal degeneration and recapitulate the features of AMD, albino rats were exposed to high intensity light for 24 h. The detailed experimental procedures were already reported in previous papers[3,4,8,9,37,41].

Nanoceria Preparation and intravitreal injection

Cerium oxide nanoparticles (nanoceria, CeO_2-NPs) were synthesized and characterized as described previously[42]. For in vivo administration, nanoceria were sterile-filtered (0.22 µm) and prepared at 1 mM in sterile 0.9% NaCl. Under anesthesia (intraperitoneal ketamine 100 mg/kg + xylazine 10 mg/kg), rats received a bilateral intravitreal injection of 2 µL of the nanoceria suspension (1 mM) in each eye using a Hamilton microsyringe with a fine gauge needle[43]. In the vehicle control group, 2 µL of sterile saline was similarly injected. Injections were performed as previously described[8–10].

RNA extraction and quality control

Seven days post-light exposure (or at corresponding time points for control animals), rats were euthanized by CO_2 inhalation and eyes were immediately enucleated. Retinas were rapidly dissected from each eye on ice. Total RNA was extracted from retinal tissue using TRIzol™ Reagent (Invitrogen, ThermoFisher Scientific) according to the manufacturer's instructions. RNA quantification was performed using the Qubit RNA HS Assay Kit (Thermo Fisher Scientific), and the RNA integrity was assessed on an Agilent 2100 Bioanalyzer (Agilent Technologies); only high-quality RNA samples with RNA Integrity Number (RIN) ≥ 7.0 were used for library preparation.

Library preparation and sequencing

For each sample, 1 µg of total RNA was processed for poly(A) + mRNA enrichment. Messenger RNA was isolated using oligo(dT) magnetic beads and converted to strand-specific cDNA. Strand-specific sequencing libraries were prepared using the Watchmaker RNA Library Prep Kit (Twist Bioscience) following the manufacturer's protocol. Adapter ligation, PCR amplification (with unique dual indexing for multiplexing), and library purification were performed as outlined in the Watchmaker workflow. Post-amplification, library quality and insert size distributions were assessed using a Fragment analyzer, confirming fragment sizes of 250–350 bp. Equimolar pools of indexed libraries were sequenced on an Illumina NovaSeq 6000 system to generate 150 bp paired-end reads, with each retina library sequenced to a mean depth of ~80 million reads. Raw sequencing data

Experimental groups	Treatment	*N*
CTRL	No treatment	6
LD	1000 lx exposure	6
VEH	Intravitreal injection of saline	6
NANO	Intravitreal injection of nanoceria	6
VEH-LD	Saline injection + 1000 lx exposure	6
NANO-LD	Nanoceria injection + 1000 lx exposure	6

Table 3. Experimental groups and treatment conditions. Summary of the six groups (CTRL, LD, VEH, NANO, VEH-LD, NANO-LD; $n = 6$ each) and interventions (light exposure, intravitreal saline, intravitreal nanoceria).

Gene	Primer Direction	Sequence (5' → 3')
Nrf2	Forward	CCAAGGAGCAATTCAACGAAG
Nrf2	Reverse	TCGTCTTTTAAGTGGCCCAA
IL6	Forward	CAAACCTAGTGTGCTATGCCTA
IL6	Reverse	TTTCAACATTCATATTGCCAGT
Sod2	Forward	GCGCTGGCCAAGGGAGATGTT
Sod2	Reverse	ATGGCCCCCGCCATTGAACTT
Actin	Forward	GCCTTCCTTCTTGGGTAT
Actin	Reverse	GGCATAGAGGTCTTTACGG

Table 4. Primer sequences used for qRT-PCR. Forward and reverse primer sequences used for quantitative real-time PCR (qRT-PCR) validation of selected differentially expressed genes (*Nrf2*, *IL6*, *Sod2*) and the housekeeping gene (*Actin*).

(FASTQ files) underwent quality control checks, including evaluation of base quality scores, GC content, and adapter contamination; all samples met predefined thresholds for downstream transcriptomic analysis.

RNA-seq data analysis

Primary analysis of RNA-seq data was carried out using a composite bioinformatics pipeline combining a canonical open-source workflow with CLC Genomics Workbench (v25.0.0) analyses. In the canonical pipeline, raw reads were first processed using fastp (v0.20) for adapter trimming and quality filtering[44]. Fastp performed per-read quality pruning and removed Illumina adapter sequences, yielding high-quality clean reads for each sample. Clean reads were then aligned to the Rattus norvegicus reference genome (e.g., Rnor_6.0) using the STAR aligner (v2.7.11) with default parameters for two-pass spliced read mapping[45]. Mapping quality was high, with the majority of reads uniquely aligned to exonic regions of the genome. Gene-level read counts were computed using featureCounts (v2.0) from the Subread package, summarizing aligned reads per gene based on Ensembl gene annotation[46]. The resulting raw count matrix was imported into R (v4.1) for downstream analysis. DESeq2 (v1.48.0) was used to normalize gene counts and identify differentially expressed (DE) genes between experimental groups[47]. The DESeq2 model accounted for biological replicate variability, and shrinkage estimators were applied to dispersions and fold changes. Shrinkage estimation of $\log_2$ fold-change ($\log_2$FC) values was performed using the apeGLM method as implemented in the *lfcShrink()* function of DESeq2 [48]. This adaptive shrinkage approach reduces variance in $\log_2$FC estimates for low-count genes while preserving effect sizes for highly expressed genes, thereby improving the reliability of differential expression calls. Volcano plots (Figs. 2A and 3A) were generated using the shrunken $\log_2$FC values, not the unshrunken Maximum Likelihood Estimates (MLE). The wide dispersion of fold-change values observed in these plots reflects the broad transcriptomic response to light damage and nanoceria treatment, with inflammatory genes showing strong upregulation and phototransduction genes exhibiting marked downregulation. Genes with a false discovery rate (FDR)-adjusted p-value < 0.05 were considered significantly differentially expressed. No fold-change cutoff was applied; all genes passing the FDR threshold were retained. Unsupervised sample clustering via principal component analysis (PCA) was performed to evaluate sample relationships and detect potential outliers. PCA results were visualized with violin plots, showing the distribution and density of sample loadings across the first three principal components (PC1–PC3), thereby highlighting transcriptional heterogeneity and treatment-specific clustering. Results from the canonical pipeline were then compared with those obtained via CLC Genomics Workbench, improving the reliability and consistency of DE findings. DE gene profiles were visualized with volcano plots and heatmaps showing the top regulated genes. To interpret transcriptomic alterations functionally, up- and down-regulated gene sets were analyzed for gene ontology (GO) and KEGG pathway enrichment using the clusterProfiler R package[49]. Enrichment testing used an FDR cutoff of 0.05. Significant GO terms (Biological Process, Molecular Function, Cellular Component) and KEGG pathways were visualized using dot plots and enrichment maps, providing insights into nanoceria-modulated biological processes in retinal degeneration. All data visualizations (PCA, heatmaps, volcano plots, enrichment plots) were generated in R using ggplot2 [50] or clusterProfiler-native plotting functions.

Real-Time PCR validation of differentially expressed genes

To validate the RNA-seq results, we performed quantitative real-time PCR (qRT-PCR) analysis on a selection of differentially expressed genes (DEGs) identified across experimental groups. Specific primer pairs were designed for key upregulated and downregulated genes, including *Nfe2l2 (Nrf2)*, *IL6*, and *Sod2* (Table 4). Total RNA was extracted from retinal tissue samples using TRIzol Reagent, followed by cDNA synthesis. qRT-PCR reactions were carried out using CFX96 Real Time System (Bio-Rad) and IQ SYBR Green Supermix (Bio-Rad) according to the manufacturer instructions. Each reaction was performed in technical triplicate. Relative expression levels were normalized to the housekeeping gene for actine, and the ΔΔCt method was used to quantify fold changes.

Statistical analysis

For non-transcriptomic measurements (e.g., nanoparticle characterization, histological quantification), data are presented as mean ± standard error of the mean (SEM), unless otherwise specified. Statistical analyses were conducted using GraphPad Prism[51] and R [52].Group comparisons were performed using appropriate parametric

tests. For comparisons involving more than two groups, one-way analysis of variance (ANOVA) followed by Tukey's post hoc test was applied. For pairwise group comparisons, unpaired two-tailed Student's t-tests were used. A significance threshold of $p < 0.05$ was employed for all statistical tests unless otherwise stated. Statistical significance for differential gene expression in RNA-seq data was assessed as described in Sect. 2.5, based on adjusted p-values calculated using the Benjamini-Hochberg false discovery rate (FDR) method.

Data availability

all relevant data generated or analyzed during this study are available from the corresponding author upon reasonable request. The raw RNA-seq data (FASTQ files) and processed count matrices have been deposited in the NCBI Gene Expression Omnibus (GEO) under the accession number GSE306375. Additional datasets supporting the findings of this study—including nanoparticle characterization data and histological images—are provided in the Supplementary Information or are available upon request from the authors.

Received: 25 August 2025; Accepted: 17 December 2025
Published online: 03 January 2026

References

1. Janaky, M. & Braunitzer, G. Syndromic retinitis pigmentosa: A narrative review. *Vis. (Basel)*. **9** https://doi.org/10.3390/vision9010007 (2025).
2. Lee, E. J. Restoration of retinal regenerative potential of Müller glia by disrupting intercellular Prox1 transfer. *Nat. Commun.* **16** (2025).
3. Fiorani, L. Cerium oxide nanoparticles reduce microglial activation and neurodegenerative events in light damaged retina. *PLoS One* **10** (2015).
4. Tisi, A. Retinal long term neuroprotection by cerium oxide nanoparticles after an acute damage induced by high intensity light exposure. *Exp. Eye Res.* **182**, 30–38 (2019).
5. Carozza, G. An overview of retinal light damage models for preclinical studies on age-related macular degeneration: identifying molecular hallmarks and therapeutic targets. *Rev. Neurosci.* **35**, 303–330 (2024).
6. Chen, J., Patil, S., Seal, S. & McGinnis, J. F. Rare Earth nanoparticles prevent retinal degeneration induced by intracellular peroxides. *Nat. Nanotechnol.* **1**, 142–150 (2006).
7. Kyosseva, S. V. & McGinnis, J. F. Cerium oxide nanoparticles as promising ophthalmic therapeutics for the treatment of retinal diseases. *World J. Ophthalmol.* **5**, 23–30. https://doi.org/10.5318/wjo.v5.i1.23 (2015).
8. Tisi, A., Passacantando, M., Ciancaglini, M. & Maccarone, R. Nanoceria neuroprotective effects in the light-damaged retina: A focus on retinal function and microglia activation. *Exp Eye Res* **188** (2019).
9. Tisi, A., Passacantando, M., Lozzi, L. & Maccarone, R. Cerium oxide nanoparticles reduce the accumulation of autofluorescent deposits in light-induced retinal degeneration: insights for age-related macular degeneration. *Exp Eye Res* **199** (2020).
10. Fiorani, L. et al. Cerium oxide nanoparticles reduce microglial activation and neurodegenerative events in light damaged retina. *PLoS One*. **10**, e0140387. https://doi.org/10.1371/journal.pone.0140387 (2015).
11. Maccarone, R., Tisi, A., Passacantando, M. & Ciancaglini, M. Ophthalmic applications of cerium oxide nanoparticles. *J. Ocul Pharmacol. Ther.* **36**, 376–383. https://doi.org/10.1089/jop.2019.0105 (2020).
12. Tisi, A. et al. Retinal long term neuroprotection by cerium oxide nanoparticles after an acute damage induced by high intensity light exposure. *Exp. Eye Res.* **182**, 30–38. https://doi.org/10.1016/j.exer.2019.03.003 (2019).
13. Tisi, A. et al. Antioxidant properties of cerium oxide nanoparticles prevent retinal neovascular alterations in vitro and in vivo. *Antioxid. (Basel)*. **11** https://doi.org/10.3390/antiox11061133 (2022).
14. Hanafy, B. *Formulation of Cerium Oxide Nanoparticles Towards the Prevention and Treatment of Cataract* (Nottingham Trent University, 2020).
15. Saraf, S. *Development of enzyme-free Hydrogen Peroxide Biosensor Using Cerium Oxide and Mechanistic Study Using in-situ spectro-electrochemistry* (University of Central Florida, 2016).
16. Tisi, A. Antioxidant properties of cerium oxide nanoparticles prevent retinal neovascular alterations in vitro and in vivo. *Antioxidants* **11**, 1133 (2022).
17. Cai, X., Seal, S. & McGinnis, J. F. Non-toxic retention of nanoceria in murine eyes. *Mol. Vis.* **22**, 1176–1187 (2016).
18. Almannai, M., Mahmoud, A., Mekki, R. A. & El-Hattab, A. W. M. Metabolic seizures. *Front Neurol* **12** (2021).
19. Chen, Y. Metabolism dysregulation in retinal diseases and related therapies. *Antioxidants* **11** (2022).
20. Aldosari, D. I., Malik, A., Alhomida, A. S. & Ola, M. S. Implications of Diabetes-Induced altered metabolites on retinal neurodegeneration. *Front. Neurosci* **16** (2022).
21. Elemam, N. M., Nader, M. A. & Abdelmageed, M. E. Ameliorative impact of sacubitril/valsartan on paraquat-induced acute lung injury: Role of Nrf2 and TLR4/NF-kappaB signaling pathway. *Naunyn Schmiedebergs Arch. Pharmacol.* **398**, 8785–8796. https://doi.org/10.1007/s00210-025-03785-w (2025).
22. He, W., Zhao, L., Wang, P., Ren, M. & Han, Y. MiR-125b-5p ameliorates ox-LDL-induced vascular endothelial cell dysfunction by negatively regulating TNFSF4/TLR4/NF-kappaB signaling. *BMC Biotechnol.* **25**, 11. https://doi.org/10.1186/s12896-025-00944-y (2025).
23. Ren, J. Long-Chain polyunsaturated fatty acids and their metabolites regulate inflammation in age-related macular degeneration. *J. Inflamm. Res.* **15**, 865–880 (2022).
24. Fang, L., Liu, J., Liu, Z. & Zhou, H. Immune modulating nanoparticles for the treatment of ocular diseases. *J Nanobiotechnology* **20** (2022).
25. Kim, Y. G. Ceria-Based therapeutic antioxidants for biomedical applications. *Adv. Mater.* **36** (2024).
26. Jung, Y. J., Tweedie, D., Scerba, M. T. & Greig, N. H. Neuroinflammation as a factor of neurodegenerative disease: thalidomide analogs as treatments. *Front Cell. Dev. Biol* **7** (2019).
27. Badia, A. Repeated topical administration of 3 Nm cerium oxide nanoparticles reverts disease atrophic phenotype and arrests neovascular degeneration in AMD mouse models. *ACS Nano*. **17**, 910–926 (2023).
28. Rutar, M., Natoli, R., Valter, K. & Provis, J. M. Early focal expression of the chemokine Ccl2 by Müller cells during exposure to damage-inducing bright continuous light. *Invest. Ophthalmol. Vis. Sci.* **52**, 2379–2388 (2011).
29. Koper, O. M., Kaminska, J., Sawicki, K. & Kemona, H. CXCL9, CXCL10, CXCL11, and their receptor (CXCR3) in neuroinflammation and neurodegeneration. *Adv. Clin. Exp. Med.* **27**, 849–856. https://doi.org/10.17219/acem/68846 (2018).
30. Nomura-Komoike, K., Nishino, R. & Fujieda, H. Effects of different alkylating agents on photoreceptor degeneration and proliferative response of Muller glia. *Sci. Rep.* **14**, 61. https://doi.org/10.1038/s41598-023-50485-7 (2024).
31. Taha, M. Activation of SIRT-1 Pathway by nanoceria sheds light on its ameliorative effect on doxorubicin-induced cognitive impairment (Chemobrain): Restraining its neuroinflammation, synaptic dysplasticity and apoptosis. *Pharmaceuticals* **15**, 918 (2022).

32. Mormone, E., Iorio, E. L., Abate, L. & Rodolfo, C. Sirtuins and redox signaling interplay in neurogenesis, neurodegenerative diseases, and neural cell reprogramming. *Front. Neurosci.* **17**, 1073689 (2023).
33. Alrobaian, M. Pegylated nanoceria: A versatile nanomaterial for noninvasive treatment of retinal diseases. *Saudi Pharm. J.* **31**, 101761. https://doi.org/10.1016/j.jsps.2023.101761 (2023).
34. Tisi, A. et al. Nanoceria particles are an eligible candidate to prevent age-related macular degeneration by inhibiting retinal pigment epithelium cell death and autophagy alterations. *Cells* **9** https://doi.org/10.3390/cells9071617 (2020).
35. Yin, Z., Kang, J., Xu, H., Huo, S. & Xu, H. Recent progress of principal techniques used in the study of Muller glia reprogramming in mice. *Cell. Regen.* **13**, 30. https://doi.org/10.1186/s13619-024-00211-z (2024).
36. Nita, M. & Grzybowski, A. Antioxidative role of heterophagy, autophagy, and mitophagy in the retina and their association with the age-related macular degeneration (AMD) Etiopathogenesis. *Antioxidants* 12, 1368 (2023).
37. Tisi, A. Nanoceria particles are an eligible candidate to prevent age-related macular degeneration by inhibiting retinal pigment epithelium cell death and autophagy alterations. *Cells* **9**, 1–17 (2020).
38. Kyosseva, S. V., Chen, L., Seal, S. & McGinnis, J. F. Nanoceria inhibit expression of genes associated with inflammation and angiogenesis in the retina of Vldlr null mice. *Exp. Eye Res.* **116**, 63–74. https://doi.org/10.1016/j.exer.2013.08.003 (2013).
39. Froehlich, T. et al. Nanobodies as novel tools to monitor the mitochondrial fission factor Drp1. *Life Sci. Alliance*. **7** https://doi.org/10.26508/lsa.202402608 (2024).
40. Huang, Y., Wang, L. & Jin, H. cRGD-Conjugated bilirubin nanoparticles alleviate dry eye disease via activating the PINK1-Mediated mitophagy. *Invest. Ophthalmol. Vis. Sci.* **65**, 55–55 (2024).
41. Tisi, A., Parete, G., Flati, V. & Maccarone, R. Up-regulation of pro-angiogenic pathways and induction of neovascularization by an acute retinal light damage. *Sci Rep* **10** (2020).
42. Passacantando, M. & Santucci, S. Surface electronic and structural properties of CeO2 nanoparticles: A study by core-level photoemission and peak diffraction. *J. Nanopart. Res.* **15**, 1785. https://doi.org/10.1007/s11051-013-1785-0 (2013).
43. Wong, L. L., Pye, Q. N., Chen, L., Seal, S. & McGinnis, J. F. Defining the catalytic activity of nanoceria in the P23H-1 rat, a photoreceptor degeneration model. *PLoS One*. **10**, e0121977. https://doi.org/10.1371/journal.pone.0121977 (2015).
44. Chen, S., Zhou, Y., Chen, Y. & Gu, J. Fastp: An ultra-fast all-in-one FASTQ preprocessor. *Bioinformatics* **34**, 884–890 (2018).
45. Dobin, A. S. T. A. R. Ultrafast universal RNA-seq aligner. *Bioinformatics* **29**, 15–21 (2013).
46. Liao, Y., Smyth, G. K., Shi, W. & FeatureCounts An efficient general purpose program for assigning sequence reads to genomic features. *Bioinformatics* **30**, 923–930 (2014).
47. Love, M. I., Huber, W. & Anders, S. Moderated estimation of fold change and dispersion for RNA-seq data with DESeq2. *Genome Biol* **15** (2014).
48. Zhu, A., Ibrahim, J. G. & Love, M. I. Heavy-tailed prior distributions for sequence count data: removing the noise and preserving large differences. *Bioinformatics* **35**, 2084–2092. https://doi.org/10.1093/bioinformatics/bty895 (2019).
49. Yu, G., Wang, L. G., Han, Y. & He, Q. Y. ClusterProfiler: an R package for comparing biological themes among gene clusters. *OMICS* **16**, 284–287 (2012).
50. *The Grammar of Graphics*. (The Grammar of Graphics, (2005).
51. GraphPad Prism version 10.5.0GraphPad Software, Boston, MA, USA, (2024).
52. R: A language and environment for statistical computing. R Foundation for Statistical Computing. R Foundation for Statistical Computing, Vienna, Austria, (2024).

Acknowledgements

The authors acknowledge support from the University of Messina through the APC initiative.

Author contributions

D.Z., R.M. and L.D. conceptualized and designed the study. M.P., V.F., M.F. and C.R. contributed to data acquisition. L.D., I.B. and D.Z. analyzed the data. L.D. and D.Z. drafted the manuscript. R.M., R.D., M.C., L.P. critically reviewed and revised the manuscript. R.M., R.D., L.P. obtained the funds. D.Z., R.M., R.D. and L.P. supervised the study.

Funding

This study was supported by the Ministry of University and Research (MUR, Italy) through the PRIN (Progetti di Rilevante Interesse Nazionale) 2022 grant (ID number: 2022PWMW5A).

Competing interests

The authors declare no competing interests.

Additional information

Supplementary Information The online version contains supplementary material available at https://doi.org/10.1038/s41598-025-33260-8.

Correspondence and requests for materials should be addressed to R.D.